Electronic Supplementary Material (ESI) for Journal of Materials Chemistry C.

One-pot Solvothermal Synthesis of lotus-leaf like $Ni_7S_6/CoNi_2S_4$ Hybrid on Carbon Fabric towards Comprehensive High-performance Flexible Non-Enzymatic Glucose Sensor and Supercapacitor

Hong Zhao[a, b], *Liping Tang*[a], *Man Zhou*[c], *Kai Li*[a], *Jinguang Hu*[b], *Yaping Zhao*[a, *], *Zaisheng Cai*[a]

[a]Key Lab of Science & Technology of Eco-textile, Ministry of Education, College of Chemistry, Chemical Engineering and Biotechnology, Donghua University, Shanghai 201620, China

[b]Department of Chemical and Petroleum Engineering, University of Calgary, Alberta T2N 1N4, Canada

[c]Key Laboratory of Science and Technology of Eco-Textile, Ministry of Education, Jiangnan University, Jiangsu 214122, China

*E-mail: zhaoyping@dhu.edu.cn

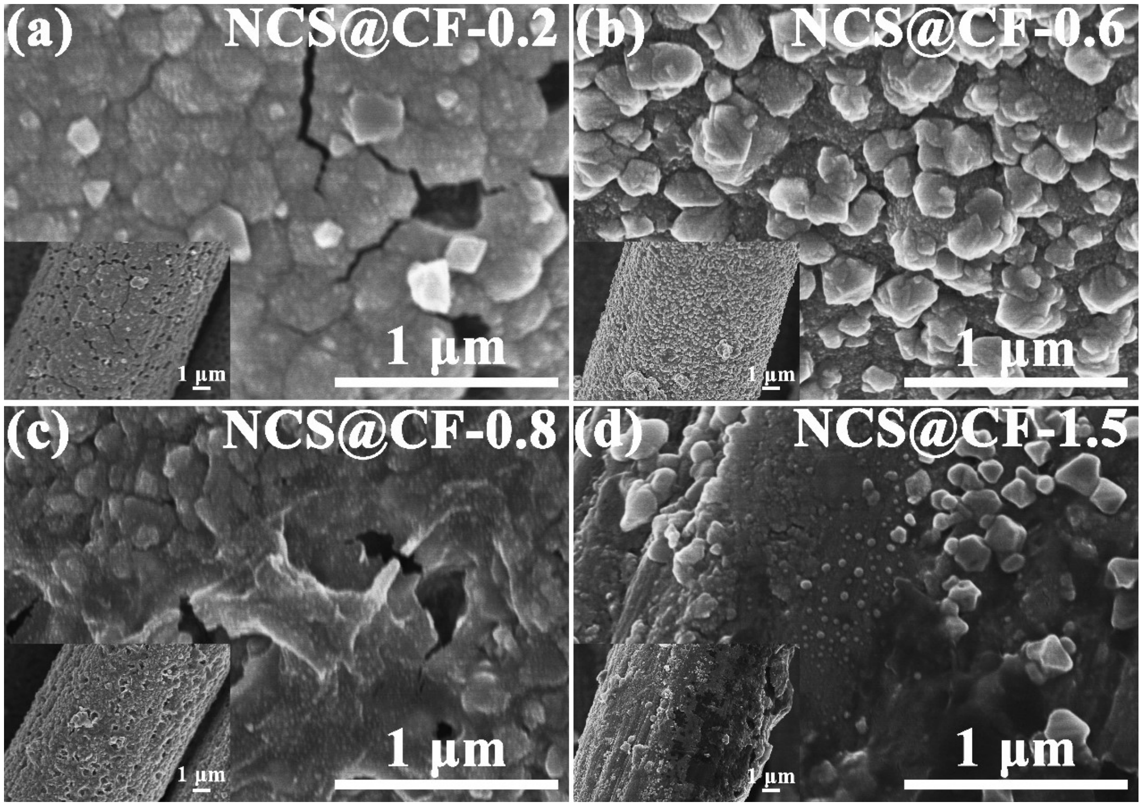

Fig. S1. SEM images at high magnification and corresponding low magnification (insets) of (a) NCS@CF-0.2, (b) NCS@CF-0.6, (c) NCS@CF-0.8, (d) NCS@CF-1.5.

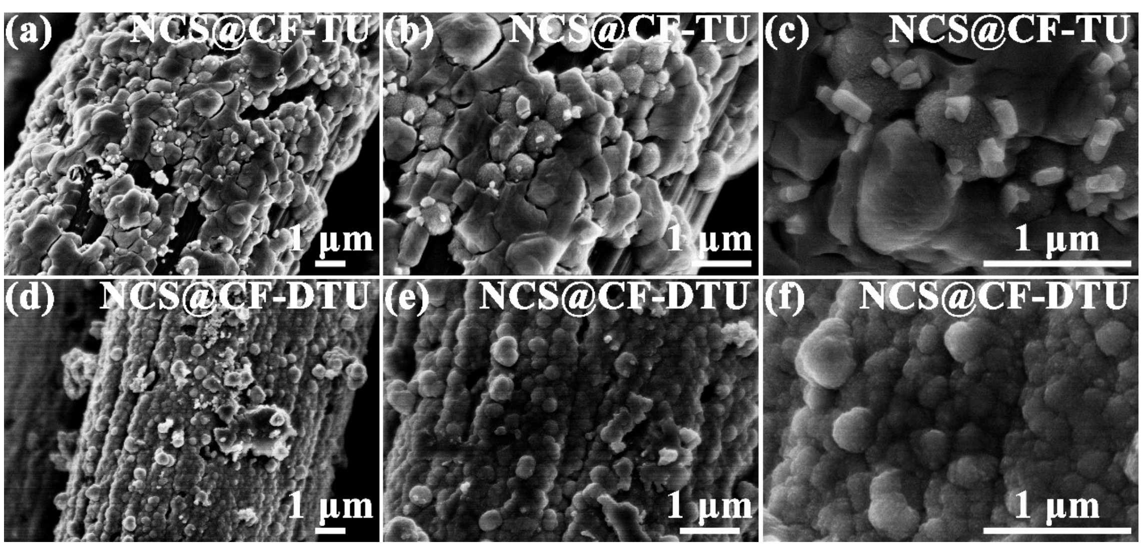

Fig. S2. SEM images of NCS@CF samples prepared with only 5.6 mM (a-c) TU and (d-f) DTU.

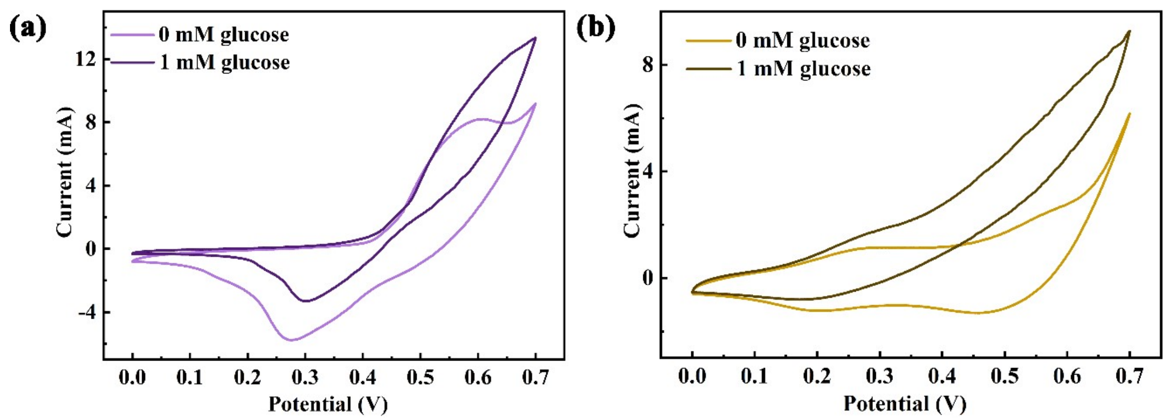

Fig. S3. The CV curves at 0.52 V of (a) NS@CF and (b) CS@CF with the present and absent of 1 mM glucose at a scan rate of 5 mV s^{-1}.

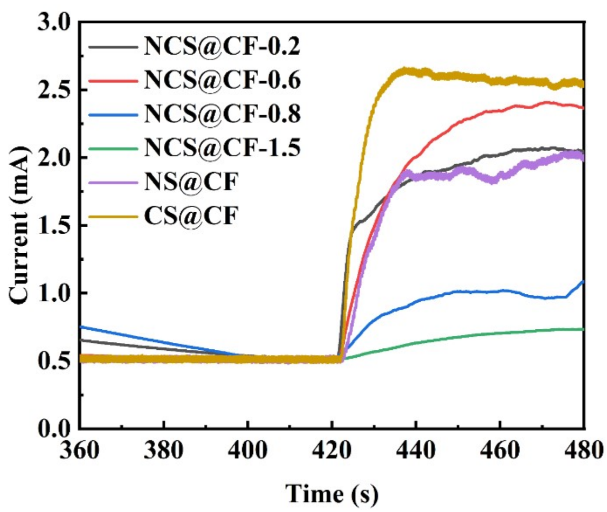

Fig. S4. The amperometric responses of NCS@CF-X (X=0.2, 0.6, 0.8, 1.5), NS@CF and (b) CS@CF.

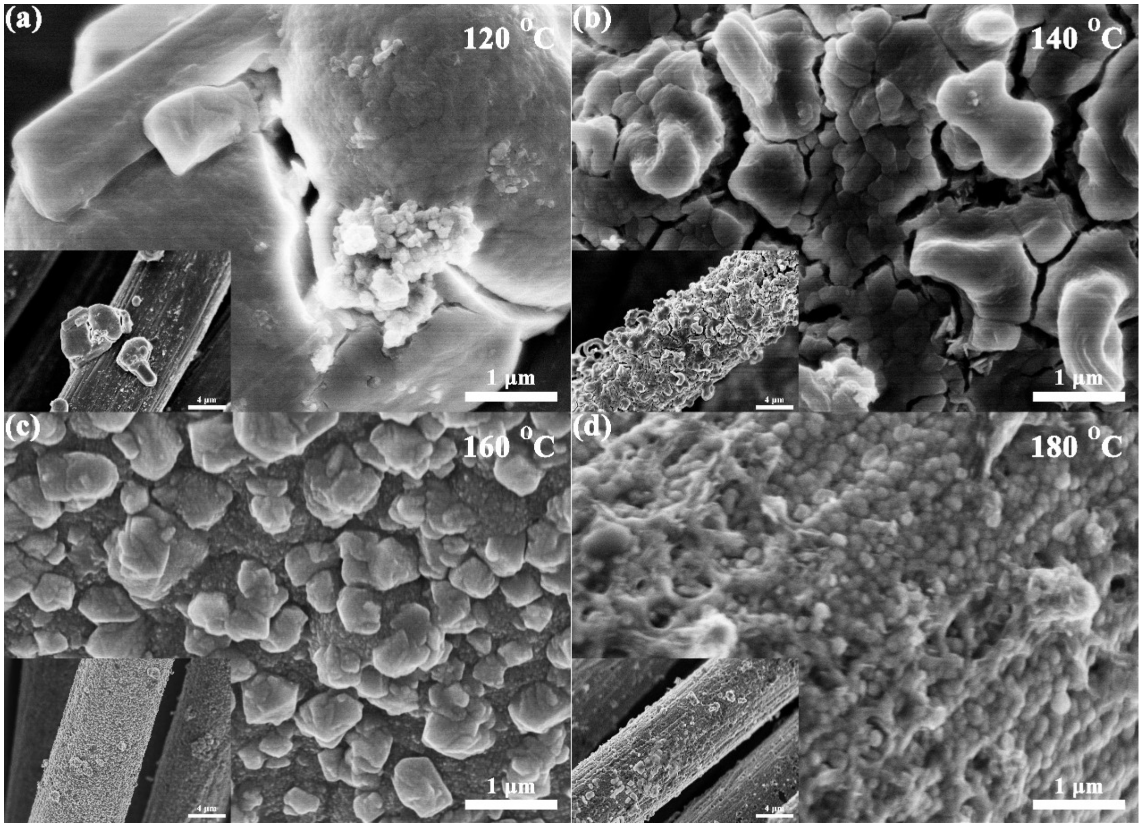

Fig. S5. SEM images at high magnification and corresponding low magnification (insets) of NCS@CF prepared under different solvothermal temperature (a) 120 ^{o}C, (b) 140 ^{o}C, (c) 160 ^{o}C and (d) 180 ^{o}C.

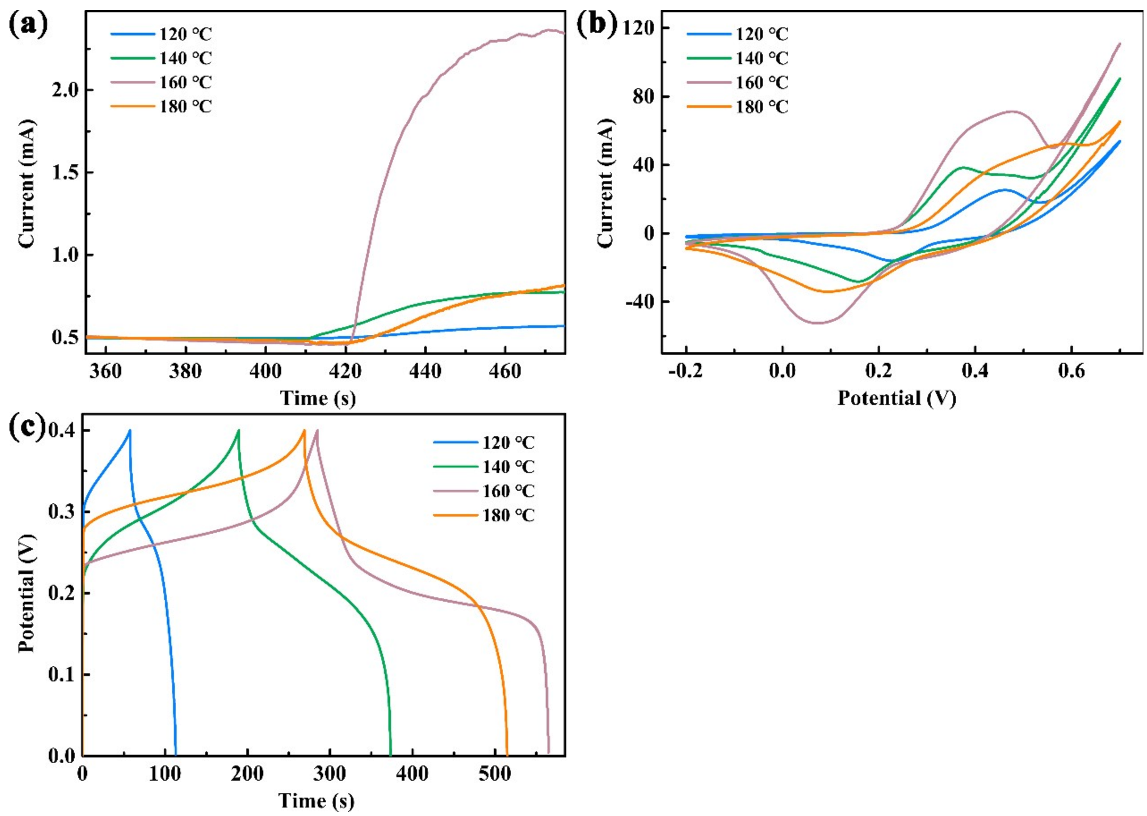

Fig. S6. (a) The amperometric responses, (b) CV curves and (c) GCD curves of NCS@CF electrodes prepared under different solvothermal temperature.

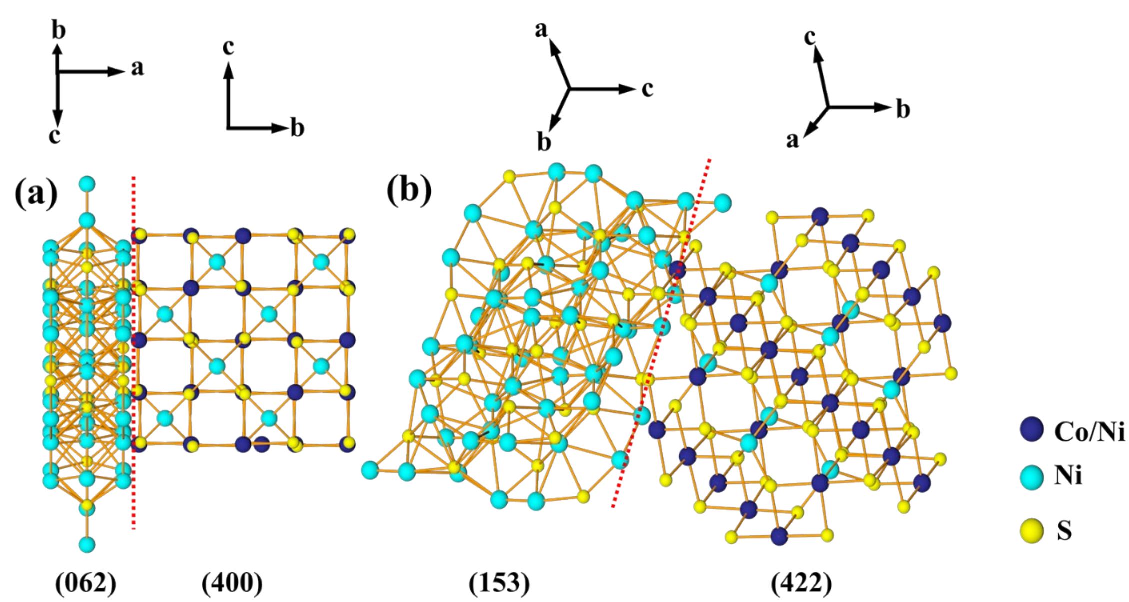

Fig. S7. Simulated crystal structure of $CoNi_2S_4/Ni_7S_6$ composite material.

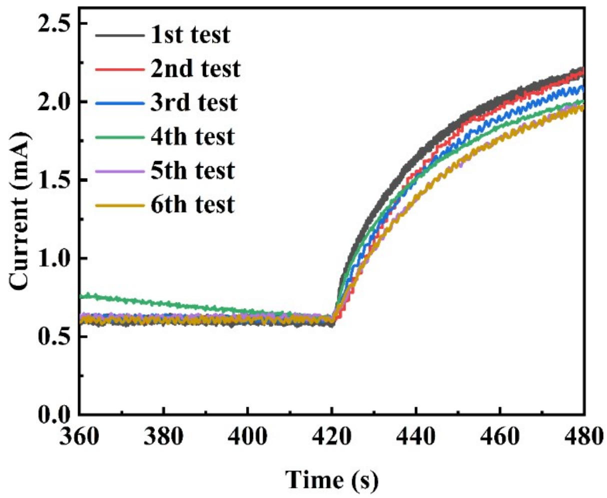

Fig. S8. Amperometric responses of the NCS@CF-0.6 towards the addition of a 0.5 mM glucose solution for respective six times.

Table S1 The Ni, Co, and S contents in NCS@CF- X (X=0.2, 0.6, 0.8, 1.5) calculated by ICP technique.

Elements		NCS@CF-0.2	NCS@CF-0.6	NCS@CF-0.8	NCS@CF-1.5
Molar (mmol)	Co	0.2512	0.2637	0.2873	0.2173
	Ni	0.5275	0.9216	1.1348	0.6519
	S	1.0368	1.4121	1.6809	1.0923
Molar ratio	Co	1	1	1	1
	Ni	2.1	3.5	3.9	3
	S	4.1	5.4	5.9	5

Table S2 Sensing performance and capacitive performance of NEGS-SC bifunctional electrodes.

NO.	Materials & morphology	Capacitive performance			Sensing performance			Ref.
		Specific capacitance	Rate capability	Stability	Sensitivity (μA mM⁻¹ cm⁻²)	Linear range response（mM）	Stability	
1	$CuCo_2S_4$ nanosheets@ carbon fiber textile	2.2 F cm^{-2} (3 mA cm^{-2})	88.2% (3~20 mA cm^{-2})	87.1% (n=3000, 32.5 mA cm^{-2})	3321.6	0.0025~3.67	95.4% (2 w)	[1]
2	Hexagonal Co_3O_4/rGO	1.69 F cm^{-2} (5 mA cm^{-2})	10% (5~10 mA cm^{-2})	80.5% (n=5000, 5 mA cm^{-2})	1315	0.001~0.5	91% (25 d)	[2]
3	3D Ni_3S_2 nanosheet @ Ni foam	2.74 F cm^{-2} (4 mA cm^{-2})	69.5% (2~10 mA cm^{-2})	91.4% (n=1000, 12 mA cm^{-2})	6148	0.005~3	-	[3]
4	yolk–shell Co_3O_4	0.77 F cm^{-2} (1 mA cm^{-2})	74.1% (1~20 mA cm^{-2})	95.8% (n=5000, 10 mA cm^{-2})	700	0.005~1.175	-	[4]
5	porous Cu_xO/Cu foil	0.16 F cm^{-2} (1 mA cm^{-2})	83% (1~12 mA cm^{-2})	-	1212.0; 852.8	0.01~0.2; 0.5~1.6	-	[5]
6	$CuCo_2O_4$ nanosheets/ITO	0.1 F cm^{-2} (2 mA cm^{-2})	10% (2~20 mA cm^{-2})	-	8.25	0.005~0.11	-	[6]
7	CuO nanotube @ Cu foil	1.1 F cm^{-2} (2.5 mA cm^{-2})	81% (2.5~50 mA cm^{-2})	95.4% (n=5000, 2.5 mA cm^{-2})	2231	0.1~3	-	[7]
	Ni_7S_6/$CoNi_2S_4$@carbon fabric	**3.9 F cm^{-2} (1 mA cm^{-2})** **3.66 F cm^{-2} (3 mA cm^{-2})**	**72.6% (1~20 mA cm^{-2})** **77.7% (3~20 mA cm^{-2})**	**100% (5000 cycles, 30 mA cm^{-2})**	**2053**	**0.0002~7.831**	**75.92% (60 d)**	**This work**

	3.50 F cm^{-2} (5 mA cm^{-2}) 3.17 F cm^{-2} (10 mA cm^{-2}) 2.84 F cm^{-2} (20 mA cm^{-2})	81.1% (5~20 mA cm^{-2}) 89.6% (10~20 mA cm^{-2})	

References

[1] W. Xu, J. Lu, W. Huo, J. Li, X. Wang, C. Zhang, X. Gu, C. Hu, Direct growth of $CuCo_2S_4$ nanosheets on carbon fiber textile with enhanced electrochemical pseudocapacitive properties and electrocatalytic properties towards glucose oxidation, Nanoscale 10 (2018) 14304-14313.
[2] A.T.E. Vilian, B. Dinesh, M. Rethinasabapathy, S.-K. Hwang, C.-S. Jin, Y.S. Huh, Y.-K. Han, Hexagonal Co_3O_4 anchored reduced graphene oxide sheets for high-performance supercapacitors and non-enzymatic glucose sensing, Journal of Materials Chemistry A 6 (2018) 14367-14379.
[3] H. Huo, Y. Zhao, C. Xu, 3D Ni_3S_2 nanosheet arrays supported on Ni foam for high-performance supercapacitor and non-enzymatic glucose detection, Journal of Materials Chemistry A 2 (2014).
[4] L. Hua, Z. Hui, Y. Sun, X. Zhao, H. Xu, Y. Gong, R. Chen, C. Yu, J. Zhou, G. Sun, W. Huang, Oxygen vacancy enriched hollow cobaltosic oxide frames with ultrathin walls for efficient energy storage and biosensing, Nanoscale 10 (2018) 21006-21012.
[5] S. Wang, L. Jiang, J. Hu, Q. Wang, S. Zhan, Y. Lu, Dual-functional CuxO/Cu electrodes for supercapacitors and non-enzymatic glucose sensors fabricated by femtosecond laser enhanced thermal oxidation, Journal of Alloys and Compounds 815 (2020).
[6] K.K. Naik, S. Sahoo, C.S. Rout, Facile electrochemical growth of spinel copper cobaltite nanosheets for non-enzymatic glucose sensing and supercapacitor applications, Microporous and Mesoporous Materials 244 (2017) 226-234.
[7] Y. Lu, K. Qiu, D. Zhang, J. Lin, J. Xu, X. Liu, C. Tang, J.-K. Kim, Y. Luo, Cost-effective CuO nanotube electrodes for energy storage and non-enzymatic glucose detection, Rsc Advances 4 (2014) 46814-46822.